

values of termolecular rate constants obtained by multiplying the capture rate of Table IV by the lifetime from Table VIII and the rare-gas collision rate from Table V, with the collision efficiencies β fixed at 0.27. As other authors have noted, stabilization of the adduct by collision with a rare gas atom does not preclude barrier crossing—indeed, stabilization by weak collisions is likely to ensure that barrier crossing occurs so that, except near the high-pressure limit, the products of the termolecular reaction are expected to be identical with the products of the bimolecular reaction.

The value of $1.82 \times 10^{-9} \text{ cm}^3 \text{ molecule}^{-1} \text{ s}^{-1}$ found for the bimolecular rate constant at 300 K is in excellent agreement with experimental values, which range from 1.6×10^{-9} to 2.2×10^{-9} . The calculated lifetime of $\text{CH}_3\text{NH}_3^{+*}$, $7.9 \times 10^{-8} \text{ s}$ at 300 K, is consistent with Saxer et al.'s experimental value of 10^{-7} s , and the termolecular rate constant $k(\text{He}) = 2.6 \times 10^{-26} \text{ cm}^6 \text{ molecule}^{-2} \text{ s}^{-1}$ is in reasonable accord with their value of 4×10^{-26} at a drift-tube energy of 0.047 eV.¹¹ It is emphasized that the calculations of Table VIII, unlike those of Table VII, contain no adjustable parameters.

Conclusions

Rate constants for various types of reaction involving CH_3^+ have been calculated over a wide temperature range with a minimum of adjustable parameters. The results obtained are in good agreement with the available experimental data and represent a fairly modest investment of time on a medium-sized computer (VAX 6210). Apart from the predictions of rate constant values at temperatures down to 10 K, and the treatment of the $\text{CH}_3^+ + \text{NH}_3$ reaction with no adjustable parameters, the main new result of this work is the conclusion that large errors can result from using the Langevin rate constant for the collision rates of complex ions with the light rare gases, and the related conclusion that helium, neon, and argon have the same collision efficiency for stabilizing adduct ions.

Acknowledgment. I am grateful to Drs. M. J. McEwan and E. E. Ferguson for helpful discussion. This work was supported by the New Zealand Universities Research Committee.

Flash Photolysis Study of 3-Methylisoxazolo[5,4-*b*]pyridine

Donato Donati,* Fabio Ponticelli,

Istituto di Chimica Organica, Università di Siena, Pian dei Mantellini 44, 53100 Siena, Italy

Paola Bicchi, and Mario Meucci

Istituto di Fisica, Università di Siena, Via Banchi di Sotto 55, 53100 Siena, Italy (Received: October 24, 1989; In Final Form: January 29, 1990)

The photoreactivity of the title compound has been examined in MeOH, PrⁱOH, MeCN, and MeCN/*as*-dimethylhydrazine solutions. A ketenimine and a spiroazirine intermediate account for the final products as well as for the transients observed in the flash photolysis experiments. It is also found that acid catalysis plays an important role in the reaction of spiroazirine to oxazolopyridine.

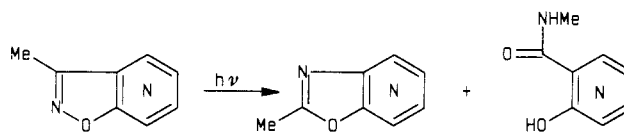
Introduction

The photochemical rearrangements of isoxazole derivatives have been known for a long time and may constitute a good starting point toward the syntheses of a number of new heterocyclic compounds provided that suitable substituents are present.¹

The main photochemical pathways that have been reported are the isoxazole-oxazole isomerization via azirine and/or via nitrilide intermediates and the ketenimine formation through the 1,2-shift of the substituent in the 3-position.² Analogous routes are found when the isoxazole nucleus is condensed with aromatic rings. In such cases, however, few data are available concerning the nature and the properties of the intermediates involved. In the case of unsubstituted benzoisoxazoles, Heinzlman and Marky³ found the 2-hydroxybenzoisocyanide as an intermediate and excluded the spiroazirine as a direct precursor of oxazole. These findings were substantially confirmed by Ferris and Antonucci using low-temperature IR evidence. Temperature effects on the yield suggested that another intermediate precedes the isocyanide.⁴

In the case of 3-methylbenzoisoxazole, Heinzlman and Marky³ attributed to a ketenimine the absorption band in the region 350–380 nm, observed in the low-temperature UV spectrum of the irradiated compound. Comparison between flash photolysis data and low-temperature IR and UV data allowed Grellmann

SCHEME I



and Tauer⁵ to attribute the transient with an absorption maximum at 350 nm to the spiroazirine generated by irradiation of 3-methyl- or 3-phenylbenzoisoxazole in polar solvents.

Following our interest in the photorearrangements of heterocyclic compounds, we studied the photoreactivity of a series of 3-methylisoxazolopyridines.¹ Irradiation of a water-saturated ethereal solution of these compounds yielded both the corresponding oxazoles and 2-hydroxypyridines or the tautomers 2-pyridones (Scheme I). These latter compounds are easily explained by water addition to the corresponding ketenimines.

In order to obtain more information on the properties of the intermediates involved in this reaction, we have undertaken a flash photolysis study of 3-methylisoxazolo[5,4-*b*]pyridine (**1**).

Experimental Section

The flash photolysis apparatus uses 50 J of discharge energy (1- μF capacitor charged at 10 kV) provided by two linear flashlamps aligned along the focal points of a bielliptical confocal cavity having a mirrorlike surface. The flash time duration (fwhh) is about 8 μs , and the analysis radiation is provided by a xenon arc lamp (Osram XBO 150 W/GS). The irradiated solution is

(1) Donati, D.; Fusi, S.; Ponticelli, F.; Tedeschi, P. *Heterocycles* **1988**, *27*, 1899, and references therein.

(2) Lang, Jr., S. A.; Lin, Y. *Comprehensive Heterocyclic Chemistry*; Pergamon Press: Oxford, 1984; Vol. 6, p 12.

(3) Heinzlmann, W.; Marky, M. *Helv. Chim. Acta* **1974**, *57*, 376.

(4) Ferris, J. P.; Antonucci, F. R. *J. Am. Chem. Soc.* **1974**, *96*, 2014.

(5) Grellmann, K. H.; Tauer, E. *J. Photochem.* **1977**, *6*, 365.

TABLE I: ¹H NMR Data of Compounds 3, 4, 6a, and 6b

compd	H ₄	H ₅	H ₆	Me	NMe	other protons	coupling constants
3	7.03 dd ^a	6.16 t	6.77 dd ^a	1.86 s	3.02 s	13.07 br (NH)	$J_{4,5} = J_{5,6} = 6.6, J_{4,6} = 1.8$
4 ^b	8.64 dd	6.31 dd	6.91 dd		2.19 s	2.47 s (NMe ₂)	$J_{4,5} = 7.4, J_{5,6} = 6.6, J_{4,6} = 1.7$
	7.07 dd	6.24 dd	7.02 dd		2.20 s	2.47 s (NMe ₂)	$J_{4,5} = 7.4, J_{5,6} = 6.6, J_{4,6} = 1.7$
6a	7.46 m ^a	6.32 dd	7.48 m ^a		2.98 s	3.76 s (OMe)	$J_{4,5} = 7.0, J_{5,6} = 6.4, J_{4,6} = 2.0$
6b	7.43 d	6.31 t	7.43 d	1.27 d	2.97 s	5.14 m (CH)	$J_{4,5} = J_{5,6} = 7.0, J_{CH-Me} = 6.1$

^a Attribution of H₄-H₆ signals may be reversed. ^b Compound 4 appears as a mixture of conformers in the ratio near 1:1, whose signals near 2.20 ppm coalesce at 47 °C ($\Delta G^* = 17.4$ kcal/mol). The attribution of NMe signals may be interchanged.

TABLE II: Kinetic Data of Decay Reactions of Intermediates A and B

solvent	A ($\lambda_{\max} = 335$ nm)			B ($\lambda_{\max} = 370$ nm)		
	$K(20$ °C), s ⁻¹	E_{att} , kcal/mol	A , s ⁻¹	$K(20$ °C), s ⁻¹	E_{att} , kcal/mol	A , s ⁻¹
Pr ⁱ OH	75 ± 2	9.70 ± 0.08	1.34 × 10 ⁻⁹	700 ± 18	11.07 ± 0.09	1.23 × 10 ⁻¹⁰
MeOH	390 ± 6	9.67 ± 0.09	7.41 × 10 ⁻⁹			
MeCN	0.6 ± 0.02	13.7 ± 0.3	3.16 × 10 ⁻⁹	10 ± 1	4 ± 0.4	1.25 × 10 ⁻⁴

contained in a cylindrical cell of 16-cm optical path length, aligned along the common focus of the bielliptical cavity. An aqueous solution of NiSO₄·6H₂O (500 g/L) surrounding the cell is used for thermal regulation and to filter the flash radiation. The transient signal is detected by a combination of a monochromator and a photomultiplier; a beam splitter in the incident light and a second photomultiplier give the reference signal to an analogic processor (SRS, Model SR235) so that the absorbance ($\log(I/I_{\text{ref}})$) is directly recorded in a digital storage oscilloscope (Hitachi VC6041). The signal is then transferred to a micro-computer for analysis. Figure 4 shows typical signals.

3-Methylisoxazolo[5,4-*b*]pyridine (**1**) was prepared and purified according to a previously reported procedure.⁶ MeOH and PrⁱOH (spectroquality grade) were treated with a small amount of sodium and distilled; MeCN (spectroquality grade) was refluxed on CaH₂ and then distilled. ¹H NMR spectra (ppm with respect to internal standard Me₄Si, J in Hz) were obtained on a Varian XL-200 spectrometer, and UV spectra were recorded with a Perkin-Elmer 124 spectrophotometer.

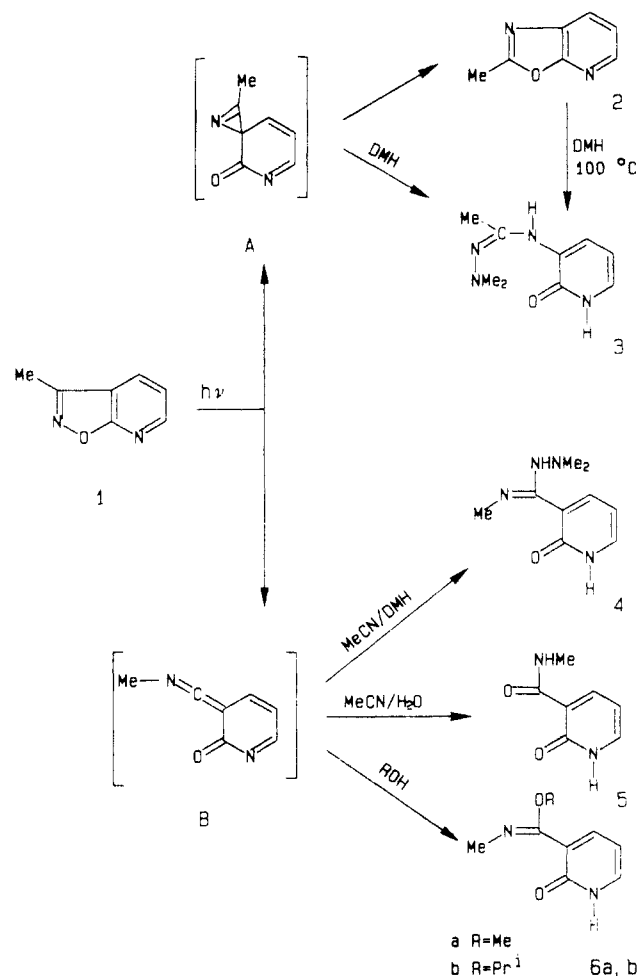
Results

Preparative Scale Experiments. Following procedures already described,¹ the behavior of **1** in MeOH, PrⁱOH, and MeCN was studied. Irradiation in protic solvents at 254 nm, followed by ¹H NMR spectra of the crude material obtained after the solvent evaporation, demonstrate that the only products are the oxazole **2** and the iminoethers **6a** and **6b** (Scheme II). Relative yields of **2/6** were 7:1 in MeOH and 10:1 in PrⁱOH irradiation. The structures of **6a** and **6b** followed from NMR data (Table I), considering the typical signals of the 2-pyridone system and the chemical shifts of N-Me and O-R protons. The reactivity of **6a** and **6b** did not permit a sufficient purification for the purpose of a quantitative UV absorption recording. Qualitative UV spectra showed an absorption maximum at 315 nm for both compounds.

In the case of irradiation of an anhydrous MeCN solution of **1**, the NMR spectra of the reaction mixture did not reveal other significant peaks except those of oxazopyridine **2** and of unreacted **1**. However, irradiation of nonanhydrous MeCN also yielded the known¹ 3-(*N*-methylcarbamoyl)-2-pyridone **5**, in the relative yield 1:9 with respect to the oxazole **2**, as determined by NMR integration. It is reasonable to suppose that both pathways are also active in anhydrous MeCN, but with the absence of protic compounds as trappers, the ketenimine resinifies in nondetectable materials.⁷

Interesting results were obtained by irradiating **1** (10⁻³ M) in a solution of *as*-dimethylhydrazine (DMH) (ca. 1 M) in anhydrous MeCN. In this case, instead of the oxazole **2**, two new products identified as the hydrazoneamide **3** and the hydrazidoimine **4** were found (relative yields of **3/4** ca. 8:1). Compound **3** was also

SCHEME II



obtained thermally by warming the oxazole **2** in DMH at 100 °C for 2 h. Considering the reactivity of the oxazoles with nucleophiles and the NMR data, the structure of **3** was determined. It is to be noted that irradiation of **2** in the same conditions as that of **1** did not yield **3**, so that we must assume that **3** was formed by reaction of DMH with a precursor of **2** whose formation was thus prevented. The formation of **4**, whose structure followed ¹H NMR data, may be explained by DMH addition on the ketenimine intermediate. Both compounds show a $\lambda_{\max} = 320$ nm in the UV absorption spectrum.

Flash Photolysis Experiments. (a) *2-Propanol Solution.* After flashing a 0.6 mM PrⁱOH solution of **1**, a strong absorption transient was detected in the range 310–390 nm. In the region 310–340 nm the transient decayed, following first-order kinetics, to a small residual absorption having a maximum at 315 nm. In the region 350–390 nm a double-exponential decay was observed

(6) Abignente, E.; De Caprariis, P.; Stein, M. L. *Farmaco, Ed. Sci.* **1975**, *30*, 992.

(7) Smith, P. A. S. *Chemistry of Open-Chain Organic Nitrogen Compounds*; W. A. Benjamin: New York, 1965; Vol. 1, p 158.

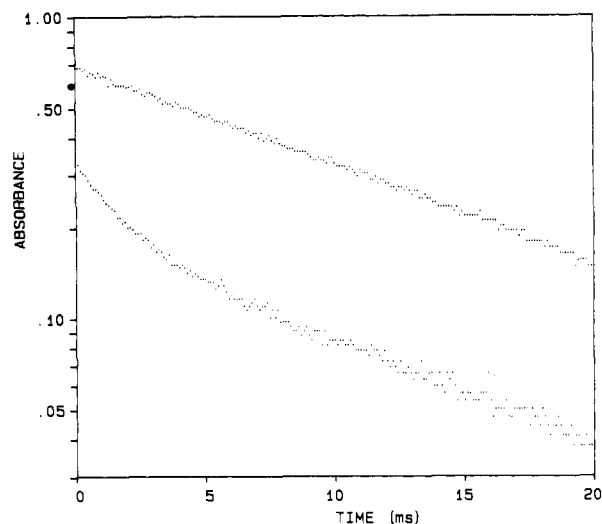


Figure 1. Transient absorption profiles obtained at 330 nm (upper curve) and 375 nm (lower curve) after flashing **1** in PrOH.

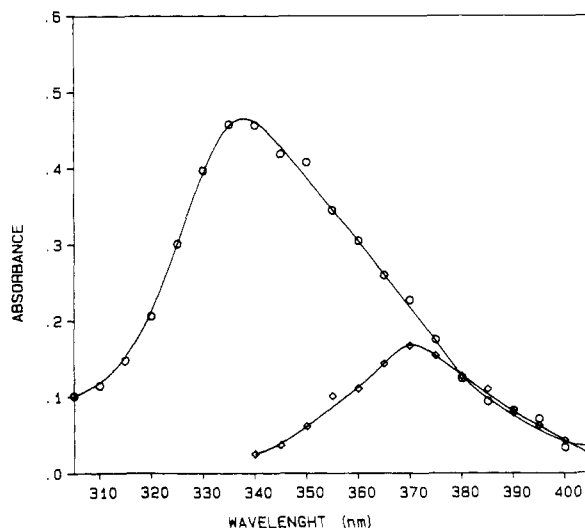


Figure 2. Absorption spectra of the two intermediates A (O) and B (◇) obtained upon flash excitation of **1** in PrOH.

without any residual absorption of the flashed solution (Figure 1). Nonlinear least-squares fitting of the decay curves allowed the determinations of rate constants (K) and absorption spectra of two transients (Figure 2). As reported in Table II, the rate constants at 20 °C were $75 \pm 2 \text{ s}^{-1}$ for the species with an absorption band centered at $\lambda = 335 \text{ nm}$ (A) and $700 \pm 18 \text{ s}^{-1}$ for that with an absorption maximum at 370 nm (B).

An Arrhenius plot of the rate constants measured at different temperatures gave activation energies of 9.70 ± 0.09 and $11.07 \pm 0.09 \text{ kcal/mol}$ for A and B species, respectively (Figure 3).

Using as solvent a 2:1 mixture of MeCN/PrOH, it was possible to evidence the rise of the absorption in the region 300–330 nm. Biexponential fitting of the transients monitored at 325 and 375 nm (Figure 4) gave for the rising exponential the same K value ($510 \pm 20 \text{ s}^{-1}$) as that of the decay of the transient with a $\lambda_{\text{max}} = 370 \text{ nm}$ (B). This information makes possible a correlation of the decay of B with the growth of the residual absorption at 315 nm and therefore with the iminoether **6b**.

(b) *Methanol Solution.* Decay transients obtained from analogous experiments on methanolic solutions of **1** were well fitted by a single exponential in the whole range examined. However, a slight dependence of the rate constants on the wavelength examined was noticed: K values changed from $390 \pm 6 \text{ s}^{-1}$ for the transient recorded at 330 nm to $500 \pm 9 \text{ s}^{-1}$ for that recorded at 380 nm. Since the preparative scale irradiation did not show any significant difference between the trend of the reaction in MeOH and that in PrOH, the single-exponential decay may be explained

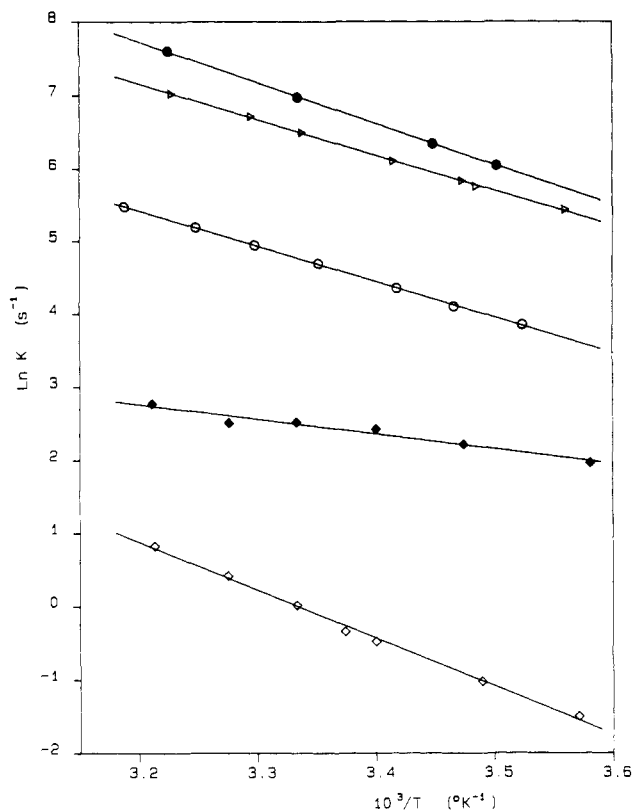


Figure 3. Arrhenius plots of the first-order rate constants for the intermediates obtained flashing **1** in various conditions: (Δ) MeOH solution, A species; (O) PrOH solution, A species; (\bullet) PrOH solution, B species; (\diamond) MeCN solution, A species; (\blacklozenge) MeCN solution, B species.

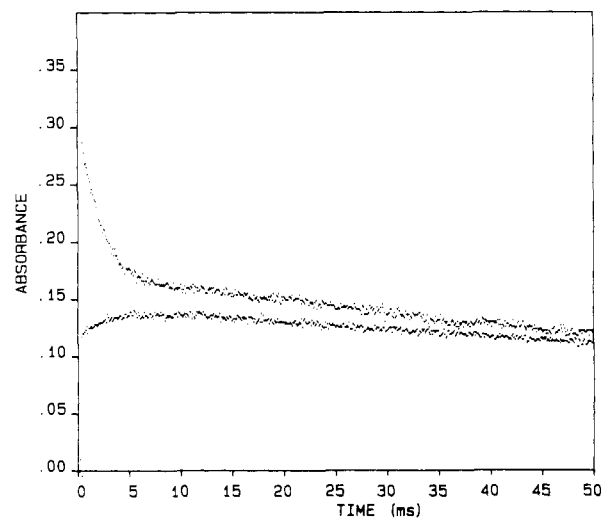


Figure 4. Transient absorption profiles recorded at 375 nm (upper curve) and at 325 nm (lower curve), after flashing a solution of **1** in a MeCN/PrOH 2:1 solution.

on the basis of a different solvent effect on the two intermediates: the rate constant of the intermediate A increases by a factor of 5 while that of B remains practically unaltered. As a result, the two rate constants become close enough to prevent the analysis of the decay curves as double exponential in the range 350–380 nm. The dependence of the rate constant on the wavelength is consistent with this hypothesis. The activation energy obtained for the A species was $9.67 \pm 0.09 \text{ kcal/mol}$, the same value, within the experimental errors, found for the reaction in PrOH (Figure 3).

The flashed methanolic solution showed a small residual absorption with a maximum at 315 nm.

(c) *Acetonitrile Solution.* Flash photolysis of a solution of **1** in MeCN revealed two long-lived transients with maxima at 330

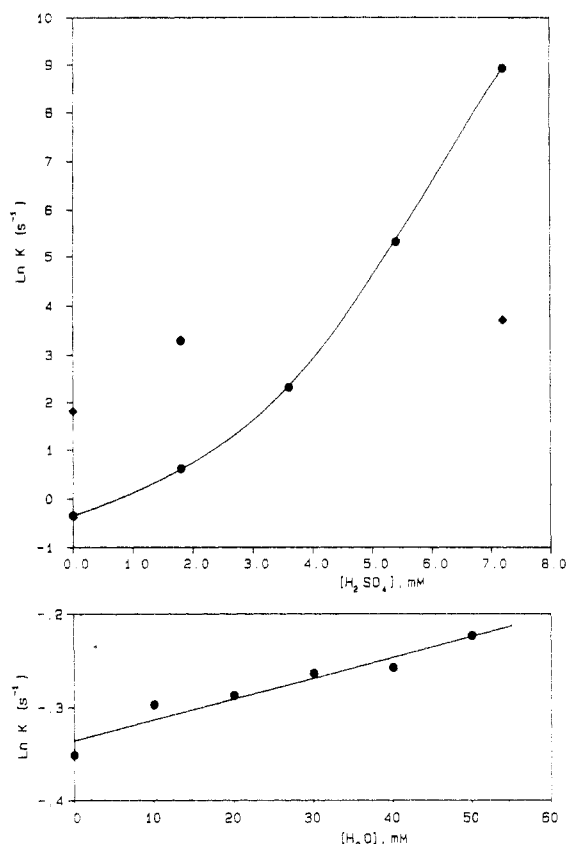


Figure 5. Dependence of the observed first-order rate constants on H_2SO_4 and H_2O concentration in MeCN: (●) A species, (◆) B species.

and 370 nm. The rate constants were 0.60 ± 2 and $10.3 \pm 1.5 \text{ s}^{-1}$; the activation energies were 13.7 ± 0.3 and $4.0 \pm 0.4 \text{ kcal/mol}$, respectively.

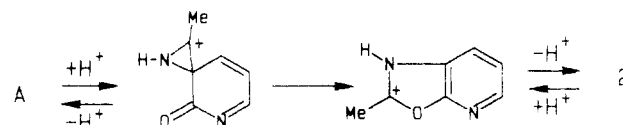
The effects of different concentrations of H_2SO_4 and of H_2O on the two transients were also examined. As shown in Figure 5, the decay rate constant of the A transient strongly depends upon the acid concentration, while the effect on the decay of B is comparably less pronounced. A small but significant increase in the decay rate of A was also observed by increasing the water concentration in the MeCN solution of **1** (Figure 5).

Finally, we carried out a series of flash photolysis experiments on a solution of **1** in MeCN in the presence of DMH, at the same concentration as that used in the preparative experiments. Only a transient with a maximum at 330 nm and $K = (2.89 \pm 0.05) \times 10^3 \text{ s}^{-1}$ was noticed. The flashed solution showed a residual absorption with a maximum at 320 nm, ensuring the correspondence between flash and preparative experiments.

Discussion

The buildup of an absorption band which peaked at 315 nm with the same rate constant as that of the decaying band which peaked at 370 nm allowed us to attribute this band to the pyridoneketenimine B (Scheme II) which, in the presence of MeOH or PrOH, adds solvent yielding the corresponding iminoethers **6a** and **6b**, whose absorption was found to peak at 315 nm. As

SCHEME III



mentioned above, the activation energy of this process was approximately 10 kcal/mol. The absorption is that expected for such a system: an analogous ketoketene showed a λ_{max} at 380 nm.⁸ In a nonprotic solvent, the ketenimine undergoes a different decay process with a different activation energy (4.0 kcal/mol).

The transient whose absorption is centered at 335 nm must be correlated with the oxazopyridine formation, i.e., with the main reaction pathways. However, a direct connection between the decay of the transient and the buildup of the oxazopyridine absorption (expected in the region 270–295 nm) could not be obtained owing to the masking presence of the residual isoxazopyridine. Taking into consideration the reported data for the benzoisoxazole photoisomerization,⁵ the spiroazirine A appears to be the most favorable candidate for this intermediate. The results obtained by irradiation of **1** in the presence of DMH are consistent with this hypothesis. In fact, addition of hydrazine on azirine with consequent ring opening has already been described.⁹ With this assumption, we have to explain the strong dependence of the decay rate constants on the nature of the solvent used, unexpected for a similar intramolecular attack. Neither polarity nor viscosity is sufficient to account for the data, in particular for the very large variation of the rate from MeOH to PrOH to MeCN without a corresponding variation in the activation energy or the effects of small quantities of water and/or of acid in MeCN solution.

In our opinion these features may be rationalized assuming that acidic catalysis by a protic solvent assists the $\text{C}=\text{O}$ attack on the spiroazirine (Scheme III): the rate constant depends upon the concentration of protonated azirine and, therefore, upon the acidity of the solvent while the activation energy, related to the ring opening of the protonated azirine, remains practically unaltered. This hypothesis accounts for the effect of the water and the acidity in the MeCN as well as for the increase of the rate for the series $\text{MeCN} \ll \text{PrOH} < \text{MeOH}$.

Previous studies have referred the acid-catalyzed addition of ketones to azirines leading to oxazolines,¹⁰ and we believe that the above mechanism also plays a very important role in the photoisomerizations of isoxazoles.

The details and generality of the acidic catalysis in the photorearrangements of isoxazoles, as well as the implications from the synthetic point of view, are currently under investigation.

Acknowledgment. The authors thank Prof. R. Bernheim for helpful discussions and kindly reading of the manuscript. Thanks are also due to Messrs. S. Bottari and E. Corsi for their technical assistance.

Registry No. **1**, 58035-50-0; **2**, 91813-42-2; **3**, 127332-22-3; **4**, 127332-21-2; **5**, 7208-83-5; **6a**, 127332-19-8; **6b**, 127332-20-1; DMH, 57-14-7; MeOH, 67-56-1; PrOH, 67-63-0; MeCN, 75-05-8.

(8) Dvorak, V.; Kolc, L.; Mich, J. *Tetrahedron Lett.* **1972**, 3443.

(9) Nishiwaki, T.; Saito, T. *J. Chem. Soc. C* **1971**, 2648.

(10) Leonard, N. J.; Zwanenburg, B. *J. Am. Chem. Soc.* **1967**, *89*, 4456.